32. Nozu T, Kondo M, Suzuki K *et al.* A comparison of the clinical features of ANCA-positive and ANCA-negative idiopathic pulmonary fibrosis patients. Respiration 2009; 77: 407–415
33. Kurata A, Nishimura Y, Yamato T *et al.* Systemic granulomatous necrotizing vasculitis in a MPO–ANCA-positive patient. Pathol Int 2004; 54: 636–640
34. Choi HK, Merkel PA, Walker AM *et al.* Drug-associated antineutrophil cytoplasmic antibody-positive vasculitis: prevalence among patients with high titers of antimyeloperoxidase antibodies. Arthritis Rheum 2000; 43: 405–413
35. Takamatsu H, Espinoza JL, Lu X *et al.* Anti-moesin antibodies in the serum of patients with aplastic anemia stimulate peripheral blood mononuclear cells to secrete TNF-alpha and IFN-gamma. J Immunol 2009; 182: 703–710
36. Matsuyama A, Sakai N, Hiraoka H *et al.* Cell surface-expressed moesin-like HDL/apoA-I binding protein promotes cholesterol efflux from human macrophages. J Lipid Res 2006; 47: 78–86
37. Popa ER, Franssen CF, Limburg PC *et al.* In vitro cytokine production and proliferation of T cells from patients with anti-proteinase 3- and antimyeloperoxidase-associated vasculitis, in response to proteinase 3 and myeloperoxidase. Arthritis Rheum 2002; 46: 1894–1904
38. Papi M, Didona B, De Pita O *et al.* Livedo vasculopathy vs small vessel cutaneous vasculitis: cytokine and platelet P-selectin studies. Arch Dermatol 1998; 134: 447–452
39. Ohlsson S, Bakoush O, Tencer J *et al.* Monocyte chemoattractant protein 1 is a prognostic marker in ANCA-associated small vessel vasculitis. Mediators Inflamm 2009; 2009: 584916
40. Kurita N, Mise N, Fujii A *et al.* Myeloperoxidase-antineutrophil cytoplasmic antibody-associated crescentic glomerulonephritis with rheumatoid arthritis: a comparison of patients without rheumatoid arthritis. Clin Exp Nephrol 2010; 14: 325–332
41. Kawakami M, Oka Y, Tsuboi A *et al.* Clinical and immunologic responses to very low-dose vaccination with WT1 peptide (5 microg/body) in a patient with chronic myelomonocytic leukemia. Int J Hematol 2007; 85: 426–429
42. Wikman A, Lundahl J, Jacobson SH. Sustained monocyte activation in clinical remission of systemic vasculitis. Inflammation 2008; 31: 384–390
43. Huugen D, Xiao H, van Esch A *et al.* Aggravation of anti-myeloperoxidase antibody-induced glomerulonephritis by bacterial lipopolysaccharide: role of tumor necrosis factor-alpha. Am J Pathol 2005; 167: 47–58
44. Bai Y, Liu R, Huang D *et al.* CCL2 Recruitment of IL-6-producing CD11b + monocytes to the draining lymph nodes during the initiation of Th17-dependent B cell-mediated autoimmunity. Eur J Immunol 2008; 38: 1877–1888

Received for publication: 28.9.2012; Accepted in revised form: 5.10.2013

Nephrol Dial Transplant (2014) 29: 1177–1185
doi: 10.1093/ndt/gfu027
Advance Access publication 24 February 2014

ORIGINAL ARTICLE

Metzincins and related genes in experimental renal ageing: towards a unifying fibrosis classifier across species

Hans-Peter Marti[1], James C. Fuscoe[2], Joshua C. Kwekel[2], Aikaterini Anagnostopoulou[3] and Andreas Scherer[4]

[1]Department of Clinical Medicine, University of Bergen, Bergen, Norway, [2]Division of Systems Biology, National Center for Toxicological Research, FDA, Jefferson, AR, USA, [3]Institute of Anatomy, University of Bern, Bern, Switzerland and [4]Spheromics, Kontiolahti, Finland

Correspondence and offprint requests to: Andreas Scherer; E-mail: andreas.scherer@spheromics.com

ABSTRACT

Background. We have previously described a transcriptomic classifier consisting of metzincins and related genes (MARGS) discriminating kidneys and other organs with or without fibrosis from human biopsies. We now apply our MARGS-based algorithm to a rat model of age-associated interstitial renal fibrosis.
Methods. Untreated Fisher 344 rats ($n = 76$) were sacrificed between 2 to 104 weeks of age. For gene expression studies, we used single colour (Cy3) Agilent Whole Rat Genome 4 × 44k microarrays; 4–5 animals of each sex were profiled at each of the following ages: 2, 5, 6, 8, 15, 21, 78 and 104 weeks. Intensity data were subjected to variance stabilization (www.Partek.com). Data were analysed with ANOVA and other statistical methods.
Results. Sixty MARGS were differentially expressed across age groups. More MARGS were differentially expressed in older males than in older females. Principal component analysis showed gene expression induced segregation of age groups by sex from 6 to 104 weeks of age. The expression level of MMP7 correlated best with fibrosis grade. Severity of fibrosis was determined in 20 animals at 78 and 104 weeks of age. Expression values of 15 of 19 genes of the original classifier present on the Agilent array, in conjunction with linear discriminant analysis, was sufficient to correctly classify these 20 samples into

non-fibrosis and fibrosis. Overrepresentation of MMP2 protein and CD44 protein in fibrosis was confirmed by immunofluorescence.

Conclusions. Based on these results and our previous work, the MARGS classifier represents a cross-organ and cross-species classifier of fibrosis irrespective of aetiology. This finding provides evidence for a common pathway leading to fibrosis and will help to design a PCR-based clinical test.

Keywords: ageing, CD44, classifier, fibrosis, matrix metalloproteinases, metzincins

INTRODUCTION

Ageing is a programmed biological process involving alteration of transcription of genes associated with many cell signalling pathways including cell survival, cell proliferation, cell transport and energy metabolism [1–3]. Such alterations of transcription results in cellular or replicative senescence increased susceptibility to apoptosis, decreased functional capacity of stem cells and progenitor cells, altered expression of growth factors, mitochondrial dysfunction and impaired regeneration and repair in the ageing kidney. This ageing phenotype leads to renal dysfunction, glomerulosclerosis, interstitial fibrosis and arteriosclerosis [4].

Fibrosis and sclerosis are the outcome of progressive chronic kidney diseases, which ultimately lead to end-stage renal disease (ESRD) requiring maintenance dialysis or kidney transplantation [5, 6]. Identification of molecular markers for renal fibrosis is of paramount clinical importance to refine current diagnosis and treatment by identification of novel therapeutic targets.

Tubulointerstitial fibrosis is characterized by proliferation and transformation of fibroblasts into myofibroblasts, deposition of fibronectin and collagens I and III into the interstitium, inflammation, microvascular rarefaction, podocyte depletion and deposition of extracellular matrix (ECM) in the interstitial space between nephrons [5]. These pathophysiological characteristics occur coincidently with the synthesis and secretion of inflammatory mediators, including interferon-γ, tumour necrosis factor-α, interleukin-1β and transforming growth factor-β (TGF-β), and members of the metzincins and related genes (MARGS) [6–8]. Within the group of MARGS, matrix metalloproteinases (MMP) are involved beyond their role as ECM-degrading enzymes in many physiological and pathological processes [9]. Examples of normal conditions are embryonic development, ovulation and wound healing [9, 10]. Important pathologic conditions with MMP involvement are inflammatory bowel diseases, arthritis, aortic aneurysms and chronic obstructive pulmonary disease [9, 11, 12]. In addition, MARGS including the TGFβ pathway and MMP play an important role in fibrosis development of solid organs and they have already been successfully used as therapeutic targets in this respect [13].

Previously we have identified a high-sensitivity, high-specificity transcriptomic classifier consisting of 19 MARGS that could discriminate human renal allograft biopsies with or without interstitial fibrosis/tubular atrophy (IF/TA) [14]. Subsequently, these classifier analyses were extended to non-transplant solid organs, such as heart, lungs, liver, kidneys and pancreas, affected with and without fibrosis [15].

The data herein are a sub-study of a larger comprehensive time-course experiment of male and female Fisher 344 rats, comprising eight age groups from 2 weeks to 104 weeks of age [2, 3, 16].

In this study, we examined age-induced alteration of renal expression of the MARGS genes, and investigated whether the previously described MARGS-based fibrosis classifier has diagnostic value across species in an experimental rat model of age-associated interstitial fibrosis.

SUBJECTS AND METHODS

Animal study

The rat in-life study, sample processing and microarray analysis were described earlier in detail [2, 3, 16]. Briefly, kidneys were obtained from the following number of Fisher 344 rats: $n = 4$ for 2, 5, 6, 8 and 104-week males; $n = 5$ for 15, 21 and 78-week males and 2, 5, 6, 8, 15, 21, 78 and 104-week females (Supplementary Table S1). These male and female (unsynchronized) Fisher 344 rats obtained from the animal breeding colony of the National Centre for Toxicological Research (NCTR) were fed the NIH-31 diet and housed under AAALAC-approved conditions with a 12-h light/dark cycle (0600–1800). Rats were treated according to the NCTR Institutional Animal Care and Use Committee guidelines (USA).

Necropsy

Animals were sacrificed at the same circadian time (between 0900 and 1100) for each time point and euthanized by carbon dioxide asphyxiation. Body weights were recorded, and kidney tissues were flash frozen in liquid nitrogen and stored at −80°C. Kidneys were collected at 52, 78 and 104 weeks of age for histological examination and placed in 10% neutral buffered formalin. Kidneys from other ages were not examined because historical data from the animal colony suggested that no fibrosis would be present.

RNA isolation

Total RNA was isolated from ∼30 mg of ground kidney using Qiagen RNeasy Mini Kit (Qiagen, Inc., Valencia, CA, USA) according to manufacturer's protocol. The yield of the extracted RNA was determined by Nanodrop-1000 (Thermo Scientific, Wilmington, DE, USA). Purity and quality of RNA were evaluated using the RNA 6000 LabChip and Agilent 2100 Bioanalyzer (Agilent Technologies, Palo Alto, CA, USA). RNA samples with RNA integrity numbers >8.0 (average of 8.7) were used.

Microarray experiments

Single colour (Cy3) Agilent Whole Rat Genome 4 × 44k microarrays were used for measurement of relative mRNA levels [3]. Full microarray data are available at Gene Expression Omnibus with accession GSE47070 (http: //www.ncbi.nlm.nih.gov/geo/query/acc.cgi?acc=GSE47070).

Microarray data analysis

Intensity files were subjected to variance stabilization including log2 transformation (www.Partek.com). Expression measures of multiple probes corresponding to a single Entrez gene were summarized as the mean value for those measures. After initial visual inspection of the data, three samples were excluded from further analysis due to suspected outlier behaviour of unknown source: Week 5 female 1, Week 15 male 5 and Week 21 male 6. One hundred and sixty-three MARGS genes are represented on the Agilent Rat Whole Genome 4 × 44k array (Supplementary Table S2). Data were analysed with ANOVA using sex and/or age as factors. Differential expression was defined as P-value ≤0.05 and |fold change| ≥1.5. Correlation of gene expression signal intensities to fibrosis grade was calculated as the Pearson correlation *r* (www.Partek.com).

Gene set enrichment analysis (GSEA) was performed as described earlier [17], and is available from www.broadinstitute.org/gsea/. Except for the MARGS list, which was assembled by the authors, gene sets were obtained from SABiosciences (www.SABiosciences.com) and are listed in Supplementary Table S2.

Pathology of rat kidney

Haematoxylin- and eosin-stained slides were evaluated for fibrosis. In all cases, the left kidney was analysed. Fibrosis was defined as an abnormal accumulation of ECM that replaces or expands/thickens normal kidney structures. The severity score of the fibrosis was based upon a grading criteria of 0–4: 0 = no increase in the amount of collagen; 1 ≤ 5%; 2 ≤ 5–35%; 3 = 36–65%; 4 ≥ 65% of the renal cortex containing an increased amount of ECM interpreted as collagen. This semi-quantitative scoring was performed by a single pathologist in a blinded fashion [3].

Immunofluorescence

Sections (5 µm) of formalin-fixed and paraffin-embedded kidney samples were used. Immunostainings for CD44 and MMP2 were performed as previously described [18, 19]. Briefly, CD44 was detected by incubating the kidney sections with mouse monoclonal anti-rat-CD44 (OX-49) antibody (554869, BD Pharmingen, San Diego, CA, USA) diluted 1:50, followed by incubation with anti-mouse secondary antibody conjugated with GFP (F2883, Sigma-Aldrich, Buchs, Switzerland, 1:100 dilution in 1× TBS).

To detect MMP2, kidney sections were incubated with goat polyclonal anti-human-MMP2 (C19) antibody (sc-6838, Santa Cruz Biotechnology, Inc., Santa Cruz, CA, USA) diluted 1:50. Thereafter, kidney sections were incubated with anti-rabbit secondary antibody conjugated with TRITC (T6778, Sigma-Aldrich, Buchs, Switzerland) in a dilution of 1:100. DAPI was utilized for nuclear staining (H-500, Vector Laboratories, Irvine, CA, USA). Fluorescence imaging was recorded in an Axiovert 200M microscope with a laser scanning module LSM 510 META (Carl Zeiss AG, Feldbach, Switzerland). DAPI was excited at 405 nm, FITCH at 488 nm and TRITCH at 588 nm.

RESULTS

Age- and sex-related differences in the expression of MARGS

Whole genome profiling of rat kidney gene expression of 4–5 animals per sex and age group was performed according to the workflow described in [2]. As we were particularly interested in expression changes of MARGS genes over time and sex, we examined 163 MARGS, which are represented on the array type used in this study, the Agilent Whole Rat Genome 4 × 44k array slide (Supplementary Table S2). Unsupervised k-means clustering was applied to identify patterns of expression across age groups (Figure 1A). The cluster analysis was performed with all age groups and sexes (16 analysis groups). Ten such clusters were chosen, as more clusters would have led to a pattern redundancy, and less would have rendered too few gene groups. Some exemplary expression profiles are shown in Figure 1B. The expression of many collagen genes decreases with age until Week 78, but slightly increases again until Week 104, particularly in male animals (clusters 1 and 2, Figure 1A), while the expression patterns of ADAMs (transmembrane proteins belonging to the zinc protease superfamily) are quite heterogeneous (compare, for example, Figure 1A, panel 3 and 10). The results of the cluster analysis by gene are provided in Supplementary Table S3.

Sex differences in age-related changes of MARGS expression

To analyse the temporal expression profile of MARGS and potential sex differences, we performed *t*-tests by sex for each age group, and filtered out those MARGS with a P-value ≤0.05 and an absolute fold change between age-matched sex groups of 1.5, which meets the recommendation by The MicroArray Quality Control Consortium [20]. In addition these genes had an ANOVA P-value ≤0.05 across all analysis groups (age and sex). As shown in Figure 2, the number of sexually dimorphic MARGS genes increases with age. While differentially expressed MARGS tend to be expressed at higher levels in females than in males in younger age groups up to ~21 weeks (with the exception of the Week 2 group), almost all differentially expressed MARGS are expressed at higher levels in males at 78 weeks and 104 weeks of age. Across all age groups 60 MARGS were differentially expressed, some of them in more than one age group.

Next we applied principal component analysis (PCA), which is a dimension reduction factor analysis method, to estimate and visualize variance in the dataset. As shown in Figure 3, the explained variance of the first two principal components (PCs) increases from 32.9% when using all unique Entrez IDs on the array (Figure 3A and B) to 43.7% when using all MARGS (Figure 3C and D). As can be seen in Figure 3C and D, MARGS expressions lead to a trend of segregation by age groups, where male and female groups follow a very similar pattern up to Week 21 and then split. Using the 60 MARGS that are differentially expressed between sexes at any time point maintained the age-dependent pattern seen with all MARGS (Figure 3E) and increased the explained

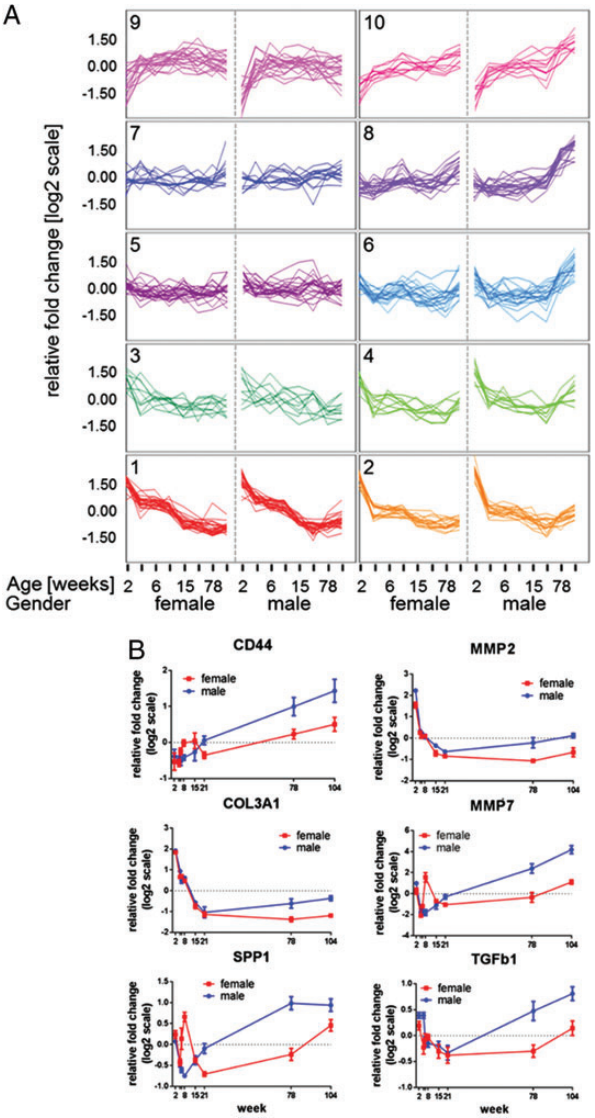

FIGURE 1: Self-organizing map clustering of MARGS genes across eight age groups and two sexes. (**A**) Clusters of co-expressed genes. *X*-axis labels for Week 5, 8, 21 and 104 were omitted due to space limitation. The normalized expression values and the assignment of MARGS genes to the clusters are provided in Supplementary Table S2. (**B**) Exemplary genes and their clusters as shown in (A): CD44 (cluster 8); MMP2 (cluster 2); COL3A1 (cluster 1); MMP7 (cluster 8), SPP1 (cluster 8); TGFb1 (cluster 6). In both (A) and (B), mean age group expression values were standardized to a mean of zero and scaled to a standard deviation of 1.

variance of PC1 and PC2 to 60.8%. The segregation of the age groups by sex becomes prominent by 6 weeks of age (Figure 3F), which may reflect sex-specific gene expression changes of MARGS after 6 weeks of age. The largest variance in the dataset comes from the factor age and is explained by PC1. PC2 appears to explain additional differences within the older age groups of Week 78 and 104. One may speculate that there is some difference in age-related factors, e.g. different grades of fibrosis. PC3 appears to explain differences in sex.

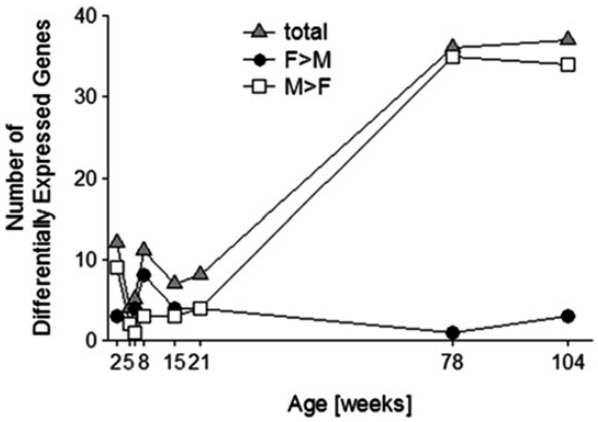

FIGURE 2: Temporal profile of sex differences in kidney expression of MARGS genes. The number of genes exhibiting a minimum 1.5-fold difference in expression between male and female animals and maximum P-value of 0.05 was calculated at each age group. In addition, these genes had an ANOVA P-value ≤0.05 across all analysis groups (age and sex). These data illustrate that the number of sexually dimorphic MARGS increases with age. Also, these sexually dimorphic MARGS are generally expressed at a higher level in males than females at older age (78 and 104 weeks).

MARGS expression in age-induced kidney fibrosis

As MARGS play a role in fibrosis, we next addressed the question whether there is a detectable relationship between MARGS gene expression and age-associated fibrosis. Pathological examinations of 20 kidneys revealed that severity of fibrosis was greater in male rats than in female rats and also severity of fibrosis increased with age (Supplementary Table S1). Four of the examined kidneys in the present study had no fibrosis (age: Week 78), 16 were positive for fibrosis (age: Week 78 and 104). Prior to Week 78, only a minority of the investigated samples displayed fibrosis grade 1 at Week 52, whereas most samples were without fibrosis at that time point (Supplementary data Table S1). Samples from Week 52 were not available for microarray analysis.

To investigate whether MARGS were significantly changed in 16 samples with presence of fibrosis in comparison to four non-fibrotic tissue specimens, we followed two analysis methods, a gene-centric and a pathway/network-centric approach. For the gene-centric approach, MARGS genes that were differentially expressed (P-value ≤0.05, fold change ≥1.5) between non-fibrotic and fibrotic samples, regardless of age, were identified. The 27 differentially expressed MARGS are shown in Figure 4A. All of them were overrepresented in samples with fibrosis. MMP7 was overexpressed by >8-fold in fibrotic kidneys, and 10 others, including CD70 and MMP25, were overexpressed by at least 2-fold. Overrepresentation of CD44 and MMP2 proteins in fibrosis was confirmed by immunofluorescence, as demonstrated in Figure 4B. Eleven of 15 collagens in the MARGS list are overexpressed in fibrosis, although not all of them met the filtering criteria for differential expression (data not shown). mRNA expression levels of MMP7 had the highest correlation to fibrosis grade, followed by TNFRSF9 and SERPINE1, as shown in Figure 4C.

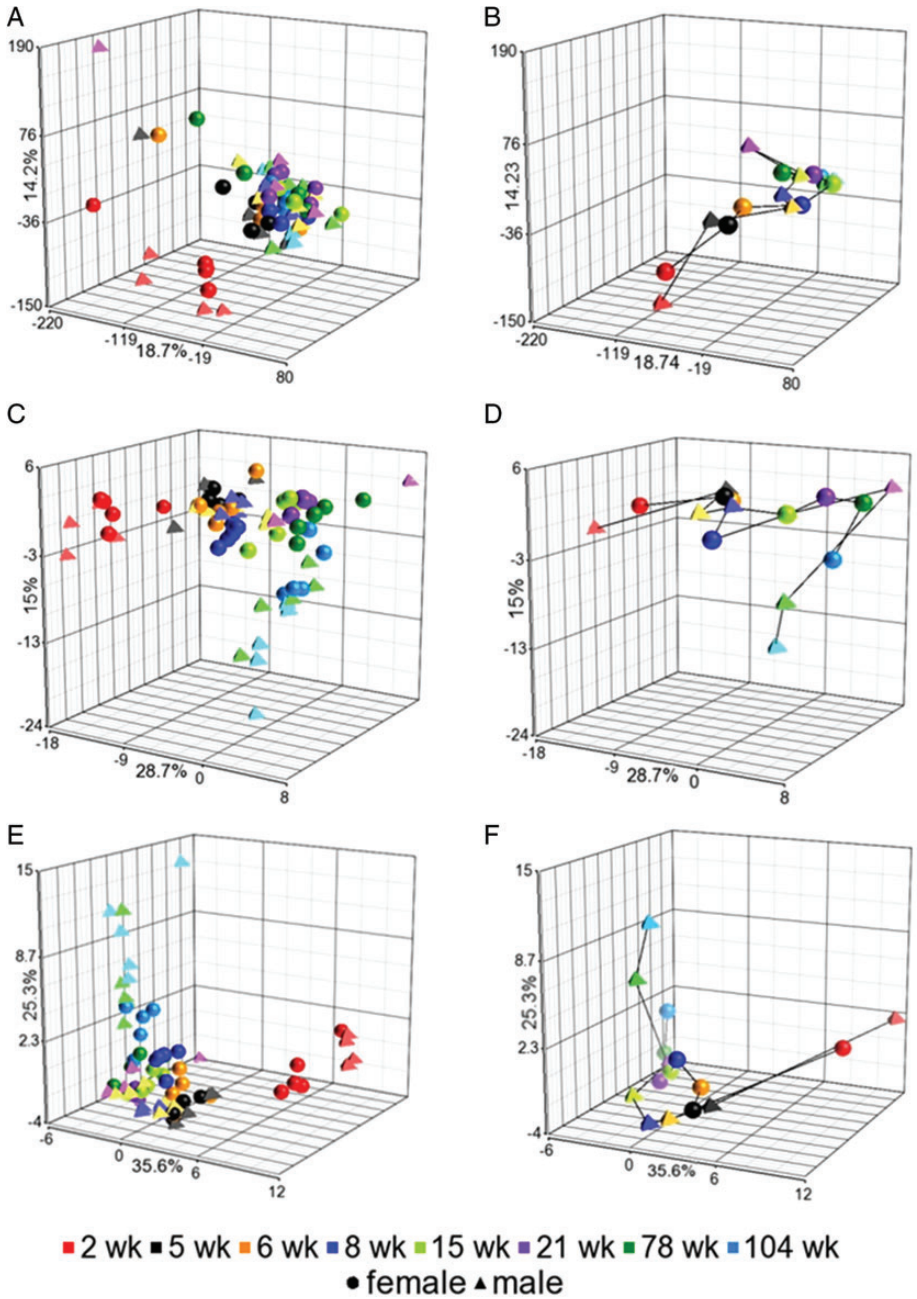

FIGURE 3: Effect of gene selection on data structure. PCA with all 17 362 unique Entrez genes represented on the array type (**A** and **B**), with all MARGS ($n = 163$) (**C** and **D**), and with differentially expressed MARGS ($n = 60$) (**E** and **F**). (A, C and E) Each symbol represents a rat sample. (B, D and F) Each data point represents the centroid of the age group corresponding to the plots on the left. The centroids of each age group are connected by sex. In each panel, a sphere represents female, a tetrahedron represents male.

A pathway- and gene-network-centric approach was applied to determine if the group of MARGS genes and other gene groups with MARGS are differentially affected during ageing. In addition to the gene set of MARGS, gene sets epithelial–mesenchymal transition (EMT), ECM, the TGF beta pathway and immune response genes were focused on (Supplementary Table S2). These were subjected to a GSEA across predefined age groups, 'young' (2 and 5 weeks old), 'adult' (15 and 21 weeks old) and 'old' (78 and 104 weeks old). As shown in Figure 5, MARGS are significantly overrepresented in young compared with old, young compared with adult and in old compared with adult. A similar trend was observed with the genes involved in EMT, ECM, TGF-β pathway and fibrosis. In contrast, immune response genes are overrepresented in old versus young, and adult versus young, and overrepresented in old when compared with adult (Figure 5).

The MARGS-based classifier of fibrosis

We next tested whether MARGS genes could serve as a surrogate marker for fibrosis in ageing rat kidneys. We previously

A

Gene symbol	p-value	Fold change (fibrosis vs control)
MMP7	0.0009	8.84
CD70	0.0021	2.67
MMP25	0.0229	2.34
TNFSF11	0.0142	2.30
SERPINE1	0.0019	2.18
SPP1	0.0001	2.15
TNFSF14	0.0358	2.10
ADAM23	0.0114	2.08
LAMC2	0.0188	2.07
TIMP1	0.0140	2.07
ADAM8	0.0273	2.00
TNFSF18	0.0280	1.94
TNFRSF9	0.0055	1.94
MMP19	0.0087	1.82
ADAMTS14	0.0436	1.79
CD44	0.0217	1.79
TNFRSF12A	0.0065	1.74
MMP2	0.0107	1.72
FASLG	0.0208	1.71
COL1A1	0.0039	1.70
LAMB3	0.0096	1.66
COL3A1	0.0091	1.63
TNFL13B	0.0237	1.59
FBN1	0.0182	1.58
TNFRSF1B	0.0133	1.55
TGFB1	0.0249	1.55
IL1B	0.0375	1.53

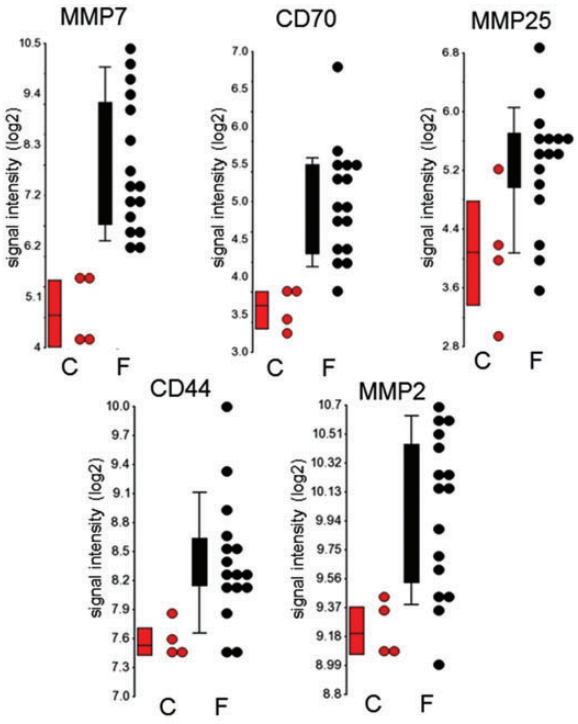

B

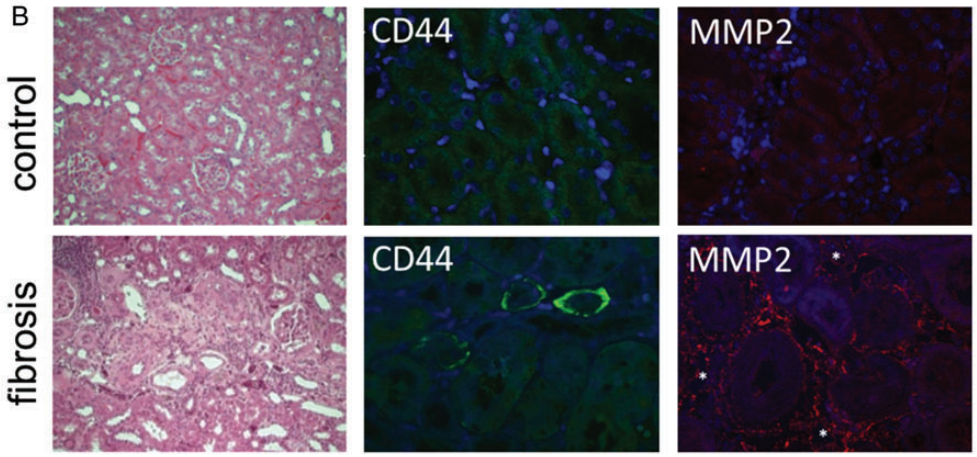

C

Gene symbol	r	P-value (correlation)
MMP7	0.7320	2.43E-04
TNFRSF9	0.7313	2.49E-04
SERPINE1	0.6954	6.63E-04
SPP1	0.6920	7.23E-04
IL1B	0.6871	8.17E-04
TNFL13B	0.6689	1.26E-03
CD70	0.6688	1.26E-03
MMP2	0.6577	1.62E-03
COL1A1	0.6505	1.90E-03

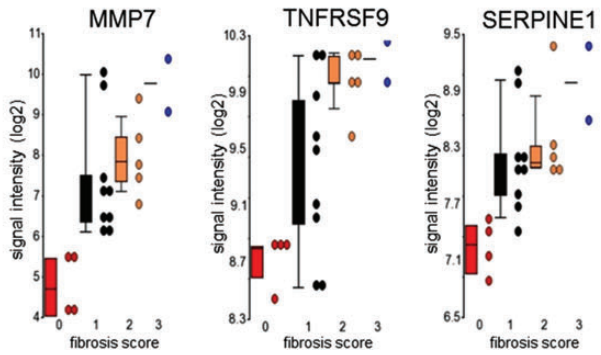

FIGURE 4: Differential expression of MARGS genes in fibrosis. (**A**) ANOVA analysis of fibrosis versus non-fibrotic samples. Twenty-seven MARGS had a P-value ≤0.05 and an absolute fold change ≥1.5. Genes were ranked by the smallest P-value and largest absolute fold change (A, left). Box plot of the three MARGS with largest absolute fold change (A, right). (**B**) Exemplary staining images of kidney fibrosis in present dataset. Left, haematoxylin stainings of control (fibrosis score = 0) = 'C', and fibrosis (score = 3) = 'F'. Centre, CD44 is overexpressed in proximal (shown) and distal convoluted tubules, glomeruli and blood vessels in renal cortex of ageing rats. Right, MMP2 is overexpressed in the cortical interstitium. Magnification: MMP2: ×63, CD44: ×40; MMP2: ×63. (**C**) MARGS with correlation $r > 0.65$ to fibrosis in 20 samples with fibrosis scores. Box plots of three MARGS with largest correlation to fibrosis scores are shown in (C), right.

Young vs old

	Size	NES	Nom P-value	FDR	
MARGS	163	1.55	0.018	0.129	UP in YOUNG
EMT	72	1.85	0.004	0.038	UP in YOUNG
ECM	71	1.44	0.11	0.149	not enriched
TGFBeta	68	1.29	0.149	0.209	not enriched
Fibrosis	73	1.16	0.258	0.259	not enriched
Immune resp.	70	1.88	0.024	0.003	UP in OLD

Adult vs young

	Size	NES	Nom P-value	FDR	
MARGS	163	1.93	0	0	UP in YOUNG
EMT	72	1.92	0	0	UP in YOUNG
ECM	71	1.73	0.01	0.014	UP in YOUNG
TGFBeta	68	1.56	0.018	0.056	UP in YOUNG
Fibrosis	73	1.53	0.012	0.055	UP in YOUNG
Immune resp.	70	1.62	0.024	0.22	UP in ADULT

Adult vs old

	Size	NES	Nom P-value	FDR	
MARGS	163	1.86	0	0.006	UP in OLD
EMT	72	1.65	0.02	0.028	UP in OLD
ECM	71	1.75	0.012	0.014	UP in OLD
TGFBeta	68	1.5	0.049	0.06	UP in OLD
Fibrosis	73	1.9	0.002	0.006	UP in OLD
Immune resp.	70	2.01	0	0	UP in OLD

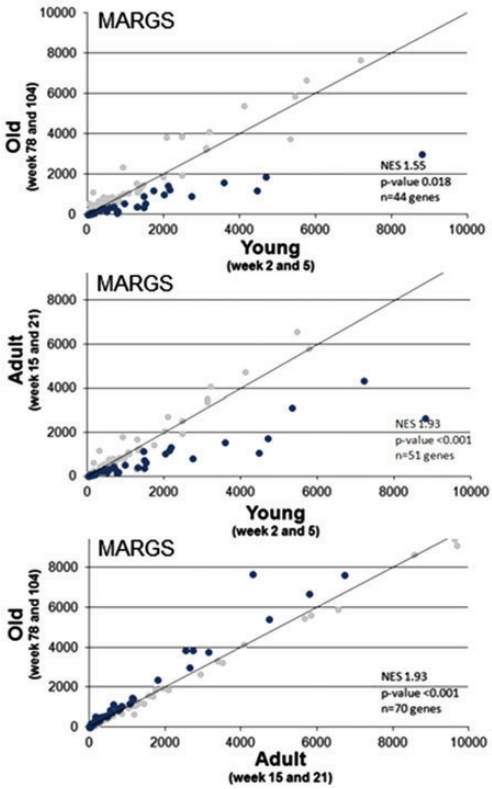

FIGURE 5: Gene set enrichment analysis (GSEA) for six gene sets with MARGS involvement. GSEA was performed with samples from 2- and 5-week-old rats ('young'), 15- and 21-week-old rats ('adult') and from 78- and 104-week-old rats ('old'). Normalized enrichment score (NES) is defined as the enrichment score divided by the mean of the enrichment scores against all permutations of the dataset. Nominal P-value is the statistical significance of an enrichment score for a given gene set. The false discovery rate (FDR) provides an estimate of the NES being a false-positive finding. The number of genes in the gene set is given under 'size'. Gene sets are provided in Supplementary Table S1. P-values and FDR <0.05 are labelled in red. The graphs on the right are scatter plots of the mean signal intensities of compared groups. Each dot represents a single gene of the gene set. Dark blue dots represent enriched genes; grey dots are non-enriched genes of the gene set.

Table 1. Performance of classifiers

Classifier panel	Fibrosis samples	Control samples	Correct classification rate (%)	Sensitivity (%)	Specificity (%)	ACC	AUC
15 MARGS genes on array	16	4	100	100	100	1	1
9 of 10 MARGS genes on array from 'minimal classifier'	16	4	100	100	100	1	1

ACC, accuracy; MCC, Matthews correlation coefficient; AUC, Area under ROC curve.

published that expression levels of a panel of MARGS genes in combination with the decision algorithm linear discriminant analysis (LDA) can serve as a classifier of fibrosis in renal tissue in humans [15]. The same classifier was applied to samples in the present study. Of 19 MARGS genes of the original classifier which was developed based on human Affymetrix HG-U133 v2 arrays, 15 genes were represented on the rat Agilent array: ADAM28, ADAMTS5, ADAMTSL3, CD44, COL3A1, EMILIN2, LAMB1, MGP, PAPLN, PLG, THBS1, THBS2, THSD1, TNFSF10 and VEGFA. Despite this limitation, all samples were classified correctly, the AUC was 1.0 and the accuracy was therefore 100%, as given in Table 1.

Previously, we also tested a composite transcriptomics classifier, which consisted of 10 of the 19 MARGS of the original fibrosis classifier [15]. This subset had been generated as a result of data integration from different array platforms taken from the literature. Ten MARGS were present on all platforms: CD44, THBS2, VEGFA, PLG, TNFAIP3, LAMB1, TNFSF10, COL3A1, THBS1 and MGP. In the present rat Agilent array, only TNFAIP3 was not represented among these 10 genes. Despite this limitation, the composite nine MARGS classifier performance in the rat ageing kidney dataset reached a significant AUC of 1 and therefore an accuracy of 100% (Table 1).

Taken together, the MARGS classifier, or a subset of it—in conjunction with the decision algorithm LDA—was sufficient to correctly classify all 20 samples with histopathology results into non-fibrosis ($n = 4$) and fibrosis ($n = 16$).

DISCUSSION

Prevalence of ESRD requiring chronic dialysis or renal transplantation continues to increase [21]. ESRD is characterized by progressive fibrosis leading to sclerosis, irrespective of its primary aetiology [22]. Accordingly, the extent of tubulointerstitial fibrosis was found to be the best predictor for kidney survival, irrespective of the underlying disease [22]. The annual cost of 1 year of dialysis treatment is >100 000 US dollars per patient in most countries. Considerable morbidity and mortality are associated with dialysis and transplantation [23, 24]. Fibrosis is difficult to treat and irreversible in the more advanced states. Thus, immunosuppressive therapy directed at underlying diseases like glomerulonephritis or vasculitis is often without benefit with respect to reversal of fibrosis. In addition, prolonged immunosuppression has severe side effects. Therefore, novel diagnostic and therapeutic strategies based on new biomarkers are necessary. To date, there are no validated transcriptomic biomarkers in routine clinical use for diagnosis of kidney fibrosis, treatment guidance or drug targets. Timely diagnosis with refined treatment indication based on biomarkers and novel therapeutic targets will greatly improve care of patients suffering from these two difficult to treat conditions. In addition, better patient care and prevention of kidney fibrosis will have implications beyond ageing for many frequent and highly relevant chronic renal diseases, such as diabetic nephropathy and hypertensive nephrosclerosis.

Recently, several novel potential fibrosis biomarkers have been identified. The miR-21 was found to be a potential novel, predictive and reliable blood marker of kidney fibrosis [25]. In another study, expression of TNFRSF6B in kidney tissues was found to be associated with renal fibrosis and to represent a biomarker for predicting the progression of chronic kidney disease [26]. In a genetic mouse model, gene expression profiling followed by biological validation identified HE4 (encoding human epididymis protein 4) as the most up-regulated gene in fibrosis-associated myofibroblasts. In that study, HE4 inhibited activity of serine proteases as well as MMP, and their capacity to degrade type I collagen. Thus, HE4, which is also elevated in serum of patients with kidney fibrosis, represents a potential biomarker of kidney fibrosis and a new drug target [27].

Especially in the Western world, the ageing population with chronic kidney diseases add to the burden of health care [28]. Thus, the investigation of age-related problems is of paramount importance in clinical practice. The ageing kidney is characterized by an augmented number of sclerotic glomeruli and interstitial fibrosis [21]. Accordingly, in our animal study, the degree of fibrosis increased with age. We have recently shown an overrepresentation of MMP2, MMP7, COL3A1, TIMP, SPP1 and other genes in fibrotic specimens of various human tissues of various aetiologies [15]. Those genes are also overrepresented in age-induced rat samples in the present study, implying that they are generally involved in fibrosis, regardless of the aetiologies and species. In addition, CD44, another member of the proposed fibrosis classifier, is differentially expressed between fibrotic and non-fibrotic samples. The expression of MMP7 and CD44, which binds a hyaluronic acid, a component of the ECM, and functions as lymphocyte homing factor and cell migration mediator [29], increases with age in both female and male rats. Others such as MMP2 and COL3A1 exhibit relatively high expression in very young renal specimens; then the expression decreases towards the adult stage and increases again towards to old age. This expression profile may be indicative of highly relevant processes of ECM remodelling during very early phases of growth, which is then alleviated during adulthood, but required again during senescence. The proteases MMP2 and MMP9 contribute to the activation of the pro-fibrogenic cytokine TGFb1 [7], whose expression also increases towards old age (Figure 1B). Previously, we have shown that MMP7 is overexpressed early in the course of interstitial fibrosis and tubular atrophy [14]. Overall, MMP7, CD70 and MMP25 are the MARGS with the highest fold-change increase in fibrosis. Not only is MMP7 the MARGS gene with the highest absolute fold change between fibrotic and non-fibrotic samples, its expression also correlated best with fibrosis grade. Thus, MMP7 may represent a biomarker for fibrosis.

Especially, the putative role of increased MMP7 in fibrosis is very much in line with a very recent and related publication demonstrating a mechanistic link between up-regulated MMP7 and fibrosis development via MMP7 mediated augmented collagen 1A2 expression [30].

Expression values of a set of genes derived from the original human fibrosis study [15], in conjunction with LDA, were sufficient to correctly classify a set of rat kidney samples—for which gene expression data and fibrosis scores were available—into non-fibrosis and fibrosis. Therefore, we have developed a classifier across species for human and murine fibrosis. Specifically, the classifier was developed based on a binominal distribution of presence and absence of fibrosis in the present and in previous publications and thus cannot be applied for different fibrosis grades or scores without further validation studies using much higher sample sizes.

After further validation in prospective studies and also based on our previously cited human studies, such a common classifier may support the putative existence of a similar final pathway of fibrosis irrespective of its aetiology and may be used for drug testing in animal models and for diagnosis of fibrosis, including judgment of prognosis. Such interventional studies would also be required to demonstrate the exact functional role and consequences of deregulated MARGS including MMP in age-related fibrosis development.

In conclusion, this MARGS classifier represents a cross-organ and cross-species classifier of fibrosis irrespective of aetiology. This finding provides evidence for a common pathway leading to fibrosis and helps to design a PCR-based clinical test.

SUPPLEMENTARY DATA

Supplementary data are available online at http://ndt.oxfordjournals.org.

ACKNOWLEDGEMENTS

This work was supported by a grant from the Novartis Foundation for Medical-Biological Research to H.-P.M. The position of Aikaterini Anagnostopoulou was funded by the European Community's Seventh Framework Programme (FP7/2007-2013) under grant agreement no. 246539. We thank the FDA Office of Women's Health for support of this project. The findings and conclusions presented in this article are the authors and do not necessarily reflect those of the Food and Drug Administration.

CONFLICT OF INTEREST STATEMENT

None declared.

REFERENCES

1. Naesens M. Replicative senescence in kidney aging, renal disease, and renal transplantation. Discov Med 2011; 11: 65–75
2. Kwekel JC, Desai VG, Moland CL *et al.* Life cycle analysis of kidney gene expression in male F344 rats. PLoS One 2013; 8: e75305
3. Kwekel JC, Desai VG, Moland CL *et al.* Sex differences in kidney gene expression during the life cycle of F344 rats. Biol Sex Differ 2013; 4: 14
4. Weinstein JR, Anderson S. The aging kidney: physiological changes. Adv Chronic Kidney Dis 2010; 17: 302–307
5. Boor P, Ostendorf T, Floege J. Renal fibrosis: novel insights into mechanisms and therapeutic targets. Nat Rev Nephrol 2010; 6: 643–656
6. Liu Y. Cellular and molecular mechanisms of renal fibrosis. Nat Rev Nephrol 2011; 7: 684–696
7. Kisseleva T, Brenner DA. Mechanisms of fibrogenesis. Exp Biol Med (Maywood) 2008; 233: 109–122
8. Farris AB, Colvin RB. Renal interstitial fibrosis: mechanisms and evaluation. Curr Opin Nephrol Hypertens 2012; 21: 289–300
9. Vartak DG, Gemeinhart RA. Matrix metalloproteases: underutilized targets for drug delivery. J Drug Target 2007; 15: 1–20
10. Arnould C, Lelievre-Pegorier M, Ronco P *et al.* MMP9 limits apoptosis and stimulates branching morphogenesis during kidney development. J Am Soc Nephrol 2009; 20: 2171–2180
11. Su BH, Tseng YL, Shieh GS *et al.* Prothymosin alpha overexpression contributes to the development of pulmonary emphysema. Nat Commun 2013; 4: 1906
12. Yamashita O, Yoshimura K, Nagasawa A *et al.* Periostin links mechanical strain to inflammation in abdominal aortic aneurysm. PLoS One 2013; 8: e79753
13. Pu KM, Sava P, Gonzalez AL. Microvascular targets for anti-fibrotic therapeutics. Yale J Biol Med 2013; 86: 537–554
14. Rodder S, Scherer A, Raulf F *et al.* Renal allografts with IF/TA display distinct expression profiles of metzincins and related genes. Am J Transplant 2009; 9: 517–526
15. Rodder S, Scherer A, Korner M *et al.* A subset of metzincins and related genes constitutes a marker of human solid organ fibrosis. Virchows Arch 2011; 458: 487–496
16. Kwekel JC, Desai VG, Moland CL *et al.* Age and sex dependent changes in liver gene expression during the life cycle of the rat. BMC Genomics 2010; 11: 675
17. Subramanian A, Kuehn H, Gould J *et al.* GSEA-P: a desktop application for Gene Set Enrichment Analysis. Bioinformatics 2007; 23: 3251–3253
18. Decleves AE, Caron N, Nonclercq D *et al.* Dynamics of hyaluronan, CD44, and inflammatory cells in the rat kidney after ischemia/reperfusion injury. Int J Mol Med 2006; 18: 83–94
19. Lods N, Ferrari P, Frey FJ *et al.* Angiotensin-converting enzyme inhibition but not angiotensin II receptor blockade regulates matrix metalloproteinase activity in patients with glomerulonephritis. J Am Soc Nephrol 2003; 14: 2861–2872
20. Consortium M, Shi L, Reid LH *et al.* The MicroArray Quality Control (MAQC) project shows inter- and intraplatform reproducibility of gene expression measurements. Nat Biotechnol 2006; 24: 1151–1161
21. Foley RN, Collins AJ. The USRDS: what you need to know about what it can and can't tell us about ESRD. Clin J Am Soc Nephrol 2013; 8: 845–851
22. Tampe B, Zeisberg M. Contribution of genetics and epigenetics to progression of kidney fibrosis. Nephrol Dial Transplant 2013; doi:10.1093/ndt/gft025
23. Kucukkoylu S, Rump LC. Cardiovascular morbidity and mortality in renal diseases. Dtsch Med Wochenschr 2013; 138: 721–724
24. Straathof-Galema L, van Saase JL, Verburgh CA *et al.* Morbidity and mortality during renal replacement therapy: dialysis versus transplantation. Clin Nephrol 2001; 55: 227–232
25. Glowacki F, Savary G, Gnemmi V *et al.* Increased circulating miR-21 levels are associated with kidney fibrosis. PLoS One 2013; 8: e58014
26. Tseng WC, Yang WC, Yang AH *et al.* Expression of TNFRSF6B in kidneys is a novel predictor for progression of chronic kidney disease. Mod Pathol 2013; 26: 984–994
27. LeBleu VS, Teng Y, O'Connell JT *et al.* Identification of human epididymis protein-4 as a fibroblast-derived mediator of fibrosis. Nat Med 2013; 19: 227–231
28. Braun L, Sood V, Hogue S *et al.* High burden and unmet patient needs in chronic kidney disease. Int J Nephrol Renovasc Dis 2012; 5: 151–163
29. Nagano O, Saya H. Mechanism and biological significance of CD44 cleavage. Cancer Sci 2004; 95: 930–935
30. Oelusarz A, Nichols LA, Grunz-Borgmann EA *et al.* Overexpression of MMP-7 increases collagen 1A2 in the aging kidney. Physiol Rep 2013; 1. doi: 10.1002/phy2.90

Received for publication: 14.11.2013; Accepted in revised form: 14.1.2014